The method of determining climatic loads on the enclosing structures taking into account global climate change

D. Y. Zheldakov and V. G. Gagarin

Research Institute of building physics of RAACS
djeld@mail.ru

Abstract. In 1997, in accordance with the UN framework Convention on climate change (UNFCCC) the Kyoto Protocol was adopted. In the Committee on adaptation (2012) States the need for all countries participating in the UNFCCC to develop national plans and programs for adaptation to conduct a technical study of the process of adaptation in different spheres and primarily in energy-intensive industries such as construction and operation of residential and administrative buildings.
Based on the numerical solution of the differential equation that determining one-dimensional heat transfer under nonsteady conditions with constant coefficients, the method of calculation of the temperature distribution over the cross section of the enclosing structure was developed. On the basis of the developed method of determining the number of cycles of freezing and thawing of moisture in the cross sections of the outer wall of the building are calculated. The developed method was tested in the experiment on the exterior walls of operated buildings. The results showed good convergence of the real and calculated temperature values. The calculation of the number of cycles of freezing and thawing on the cross section of the outer wall of the building according to the developed methodology and the experiment showed the same results.
The method of numerical assessment of the impact of global climate change on the enclosing structures was developed. The concept of temperature intensity of the year was introduce. The method uses meteorological data of outdoor air temperature for the previous period and the results of calculation of temperature regime of the enclosing structures.
The use of this method allowed to calculate the number of cycles of freezing and thawing in cross sections of the outer wall at any time interval, and, therefore, more accurately predict the durability of the enclosing structures.

Keywords: climate changes, durability, the building envelope, method of calculation.

1 Problem Statement

When developing the method for calculating the maximum durability (life cycle) of various enclosing structures, i.e. determining the period, during which an enclosing structure performs its functions, it is necessary to assess correctly the rate of the enclosing structure material destruction. In the high latitude, the main criterion of material resistance to destruction is its freeze-thaw resistance. The process of polythermal crystallization leading to the destruction of material of the external building wall is the counting function of the number of cycles of structure material temperature transitions through zero.

The process of freezing and thawing goes not only on the surface of the material external wall but in the depth of it, which results in the strength decrease and even material destruction in the external wall cross-sections at a certain distance from the surface. The decrease of structure material strength reduces the strength of enclosing structure in general. That is why knowing the exact number of cycles of temperature transitions through zero in every cross-section of the external enclosing structure is necessary to determine the maximum durability (life cycle) of the external building wall.

To estimate the number of cycles of temperature transitions through zero in various cross-sections parallel to enclosing structure external surface, it is necessary to resolve the matter of temperature waves passing the wall at outdoor air temperature fluctuations, i.e. to calculate the temperature distribution over the wall mass under nonsteady conditions.

However, the task of developing the method for determining the number of freezing and thawing cycles should be stated and resolved at a broader level. In the calculations, it is necessary to consider the global climate change and, therefore, the climatic component should be introduced into the calculation method along with the thermotechnical component,

The Kyoto Protocol adopted in 2005 in accordance with the UN Framework Convention on Climate Change (UNFCCC) and materials of the committee on adaptation suggest that all the UNFCCC countries are to develop the national plans and programs for adaptation, including development of areas and promotion of programs on assessment of impact, vulnerability, and adaptation to the climate change, first of all, to the growth of outdoor air temperature, and to conduct a technical study of the process of adaptation in different spheres in 2016-2020 [1-3].

One of the main areas of programs for adaptation to global warming is studying the impact of varying environmental parameters on structural materials durability. This conditions the necessity of developing new methods for calculation of climatic impact on strength and durability of enclosing structures taking into account both the temperature change, and the number of cycles of temperature transitions through zero, as the part of the program on adaptation to the climate change or the buildings and structures durability.

On Figure 1 the graphs are shown that characterize the warming both at the global level of the planet climate change and at the territory of Russia and, more specifically, at the territory of Moscow as a metropolis. Starting from the middle of XX century, the annual average temperature increase in Moscow has been more substantial than that on the average throughout the planet. Along with the average annual temperature increase, the number of cycles of outdoor temperature transitions through zero grows. On Figure 2 the calculations are given regarding cycles of temperature transitions through zero as per the results of observations in Moscow since 1966 till 2016 made by the authors. It should be noted that the graph slightly tends towards the increase of the number of cycles of temperature transitions through zero, however the joint consideration of the graphs shown on the Figures 1 and 2 sets the trends of outdoor air characteristics.

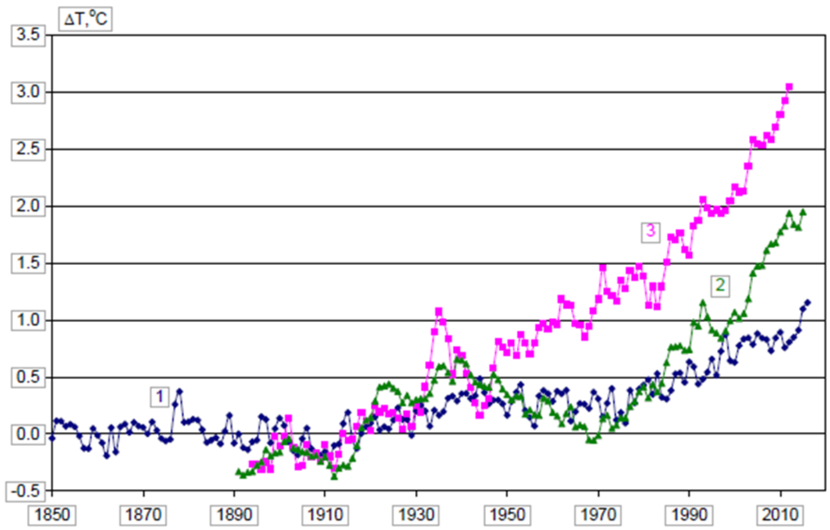

Fig. 1. Changes in average annual temperature of the surface layer of air ΔT in 1850 to 2015, the average for the planet (1) according to [4], on the territory of Russia (2) and in Moscow (3) according to [5].

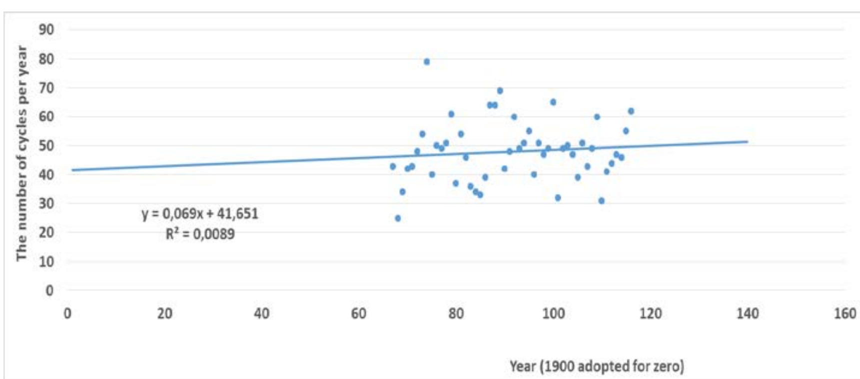

Fig. 2. The Number of cycles of the zero crossing of outdoor air temperature in Moscow (according to data from 1966 to 2016)

The climate parameters [6,7] considering standards that are currently in force in Russia describe the temperature fluctuations in winter and summer season with such parameters as mean monthly values of air temperature in January and July as well as the coldest (hottest) day temperature departures from average monthly values. These parameters do not allow reflecting the climatic changes as they operate with average calculated values. The use of "typical year" parameters in the calculation does not make it possible to consider the trends of outdoor air characteristics change as well, because leveled annual data are used for forming the "typical year" characteristics. Similar standards are in force in other countries of the world as well.

Receiving the reliable results on the number of freezing and thawing cycles over the cross section of external enclosing structure is important for the analysis of the structure durability and for the possibility to calculate its life cycle. Thus, the problem shall be stated in the following way: it is necessary to develop the method of calculating the number of cycles of freezing and thawing of enclosing structure that would allow to determine the number of cycles of freezing and thawing in any cross-section of the brickwork considering moisture and solar irradiation. At that, the developed method should allow considering the global climate change in any region.

2 Calculation Method

Method of calculating the number of cycles of freezing and thawing of enclosing structure in any brickwork cross-section considering the global climate change consist of several stages. At the first stage, the problem is solved on temperature distribution over the brickwork section under nonsteady heat transfer conditions for one-dimensional heat flow. At the second stage, the corrections are introduced into calculated data for considering the structure moisture and, therefore, the heat consumption for ice formation and melting in the structure, the solar irradiation influence on calculated outdoor temperature, the temperature of freezing and thawing commencement is adjusted in accordance with the chemical composition of electrolyte inside the brick fragment. At the third stage, based on the statistical analysis of calculated data on the number of freezing and thawing cycles in various sections of enclosing structure, the schedules of change in the number of freezing and thawing cycles in each cross section are defined, which makes it possible to identify the number of freezing and thawing cycles during any time interval considering the global climate change in any region and for any structure. This article described the method itself in brief, as the main focus is on the analysis of results and possibility of estimating the design solutions of enclosing structures from their durability viewpoint.

2.1 Method for Calculating Temperature Distribution Over Brickwork Cross-Section

The problem of temperature distribution over the brickwork cross section is resolved on the basis of the mathematical solution for the one-dimensional problem of nonsteady process, when heat is transferred via the flat wall with indefinite length proposed by O.E. Vlasov [8] and K.F. Fokin [9]. To resolve the set problem of the temperature distribution over the cross section of external enclosing structure it is necessary to solve the Fourier's differential heat equation that defines the one-dimensional heat transfer under nonsteady conditions

$$\frac{\partial t}{\partial z} = a\frac{\partial^2 t}{\partial x^2} \quad , \tag{1}$$

where a – 'thermal diffusivity coefficient, m^2/s;

$$a = \frac{\lambda}{c\gamma} \quad , \tag{2}$$

where λ - thermal conductivity of material, $W/(m^2\,{}^oC)$; c - specific thermal capacity of material, kJ/(kg K); γ - material density, kg/m^3; t - temperature, ^oC; z - time, s; x - coordinate along heat transfer axis, m.

The boundary conditions of the third kind for the inner surface of the wall is the law of heat transfer between the wall and the internal environment with t=20 °C.

The general formula for defining the temperature in any plane after the time interval Δz per the temperatures in the same plane and in two proximate planes in the previous moment z shall be as follows:

$$t_{n,z+1} = t_{n,z} + a\frac{\Delta z}{\Delta x^2}\,(t_{n+1,z} + t_{n-1,z} - 2t_{n,z}) \tag{3}$$

This scheme is today recognized as Crank-Nicolson scheme [10-16].

The initial temperature distribution over the wall cross section is calculated based on the assumption that as of the beginning of calculation the steady conditions have been reached in the wall.

For reliable sampling, the graphs were plotted regarding temperature distribution in the given cross sections since October 1966 till April 2011. The reference year was taken since the month, when the outdoor air temperature was below zero degrees, till the month, when no temperature below zero was recorded. Thus, in the period under consideration about 600 000 reference points were obtained, based on which 2450 graphs of temperature distribution over brickwork cross section were plotted.

On Figure 3 the results of temperature distribution over the cross-section of the external building wall are shown. The graphs of outdoor temperature, external surface temperature and temperature in the relevant cross-sections of the brickwork are shown on the Figure. The number of cycles of temperature transitions through zero in any cross section of brickwork shall be determined by the double crossing of the horizontal line corresponding to zero degrees. Calculation results for the entire basic reference period since October 1966 till April 2011 are summarized in the Table 1.

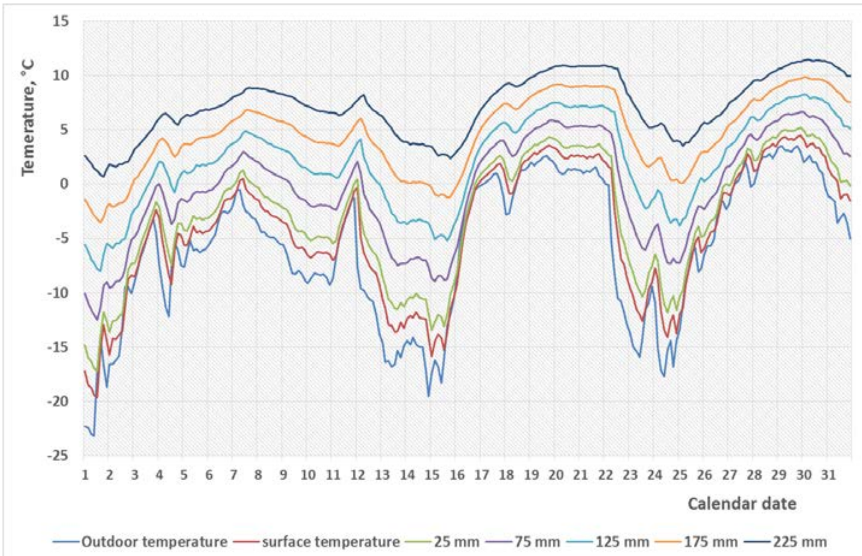

Fig. 3. The temperature distribution over the cross section of the external wall (brick 510 mm) in December, 1998.

Table 1. Number of transitions through zero over the cross-section of the external wall of the building (510 mm solid bricks) per months (Number/percent of total transitions in this cross-section).

Designed cross-section of external wall	Month										Total ransi-tions in this cross-section
	VIII	IX	X	XI	XII	I	II	III	IV	V	
outdoor temperature	2	38	283	301	249	214	256	639	395	21	2398
surface temperature	1	10	137	223	242	196	218	490	156	4	1677
25 mm	0	6	77	175	222	184	206	424	71	1	1366
		0,44	5,64	12,81	16,25	13,47	15,08	31,04	5,20	0,07	
75 mm	0	0	22	103	185	159	203	259	8	0	939
			2,34	11,14	19,70	16,93	21,62	27,59	0,85		
125 mm	0	0	1	51	137	153	227	141	0	0	710
			0,14	7,18	19,30	21,55	31,97	19,86			
175 mm	0	0	0	16	65	111	134	12	0	0	338

				4,73	19,23	32,84	39,65	3,55			
	0	0	0	1	11	31	22	0	0	0	65
225 mm				1,54	16,92	47,69	33,85				

The developed method allows to calculate the temperature distribution over the brickwork cross-section under nonsteady conditions not only in case of outdoor temperature change but also considering the change of the indoor temperature.

2.2 Experimental Verification of Developed Calculation Method

Field experiment was conducted to verify the accuracy of the developed heat distribution calculation method at a cross-section of the external building wall. For the experiment, the building constructed in 1905 was chosen, with 950 mm thick external walls made of solid loan brick. The wall, on which the experiment was conducted, was oriented to the south orientation and faced a closed yard. The nearest building wall is located 4.7 meters away [17-18].

To measure temperature and heat flow density, the device was used for measuring and logging the heat flow rate going through heat exchange surfaces of thermal power facilities as well as temperature of those surfaces and their surrounding gaseous and granular medium. Measurement range for heat flow density is 10 – 999 W/m^2, for temperature -30 – 100 ^{o}C.

Device operating principle involves the measurements of thermo-electromotive force of temperature sensitive heat flow sensors and temperature sensors resistance.

Temperature sensitive sensors consist of galvanic copper–constantan thermobattery made of several hundred thermocouples connected in series, bifilarly folded down in spiral and filled with epoxy compound with various additive agents. The sensor has two outputs (one on each side of the sensitive element). Sensor function is based on "additional wall" principle. The sensor is fixed on heat transfer surface of the subject forming an additional wall. Heat flow going through the sensor forming a temperature gradient and a corresponding thermoelectric signal inside it.

Platinum themoresistance sensor locked in a leak-tight disk-shaped case are used as remote temperature sensors in the device; they provide for measuring surface temperature of solid bodies by way of fixing (sticking) them to the studied surfaces, and for measuring air and granular media temperature by way of immersion.

Temperature sensors were installed for measuring outdoor (t_1) and indoor (t_7) temperature at the distance of 300 mm away from the wall surface, external (t_2) and internal (t_6) wall surfaces temperature, and three sensors were installed inside the external wall at the distance of 85(t_3), 185(t_4) and 280(t_5) mm from external wall surface (Figure 4).

During the installation process of (t_3) - (t_5) sensors several holes of 22 mm were drilled on the internal wall surface. Sensors were installed on the end surface of the drilled hole using thermal compound and fixed with a special device. Open end of the holes was insulated at 150 mm depth using an insolent. Three heat flow sensors (q_1, q_2, q_3) were installed on the inner surface 250 mm apart from one another. The arithmetic average of the readings was taken as the heat flow value.

The experiment was performed for over 3.5 months, since early January till mid-April. The interesting feature of this period is that during it the lowest temperatures of outdoor air and the period of active temperature transition through zero were recorded. During the field experiment in automatic mode, every twenty minutes outdoor (t_1) and indoor (t_7) temperature, temperature of external (t_2) and internal (t_6) wall surfaces was measured, as well as heat flow values at three points (q_1, q_2, q_3). The arithmetic average of three readings was taken as the heat flow value.

Real values of material thermal conductivity coefficient of external wall as well as heat transfer coefficient of the internal and external surfaces were calculated on the basis of those values. Besides, heat conduction coefficient was calculated based on the temperature values t_3 and t_5 in cross-sections at 85 and 280 mm depth from the external surface. The calculation results demonstrated the good convergence: the average values of two calculations were 0.85 and 0.88 W/(m K). Further, the calculations of heat transfer coefficient of external and internal walls were made. Due to the massive amount of experiment data, the Figure 5 demonstrates the results of experiment and interim calculated values for 16 days, since 4th till 20th of January 2017.

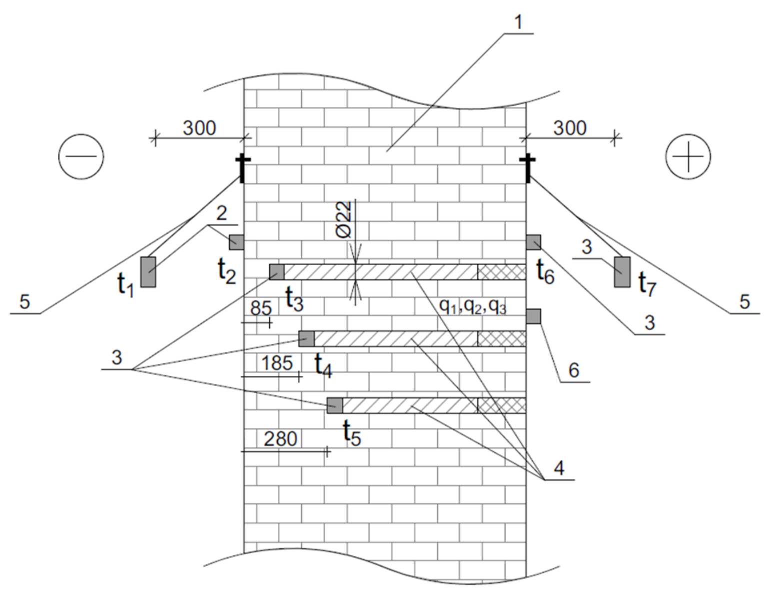

Fig. 4. The arrangement of sensors for experimental confirmation of the calculation of the temperature distribution over the cross section of the outer wall.

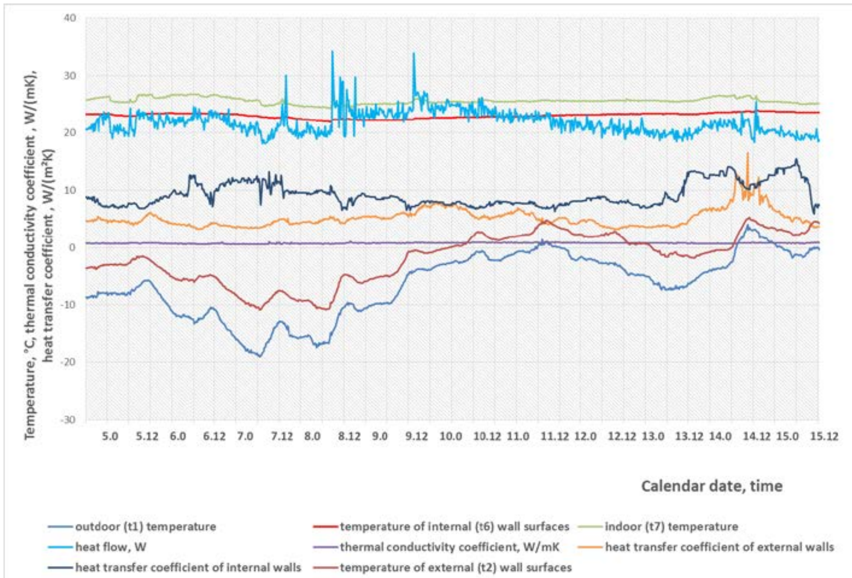

Fig. 5. Experimental data of the temperatures of external and internal air, temperatures of internal and external wall surface and the calculated values of heat transfer coefficients and thermal conductivity coefficient.

The thermal conductivity was calculated as per the formula (4)

$$\lambda = \delta q/(t_6 - t_3) \tag{4}$$

where δ - wall thickness, m; q - average heat flow value, W/m^2; t_6, t_3 - temperature of internal surface of the wall and at the depth of 85 mm from external surface, ^{o}C.

To verify the solution, the heat conduction coefficient was calculated based on the temperature values t_3 and t_5 in cross sections at 85 and 280 mm depth from the external surface. The calculation results demonstrated the good convergence, the graphs λ_1 m λ_2 were almost identical. The average values of two calculations were 0.83 and 0.88 W/(m ^{o}C).

Further, the calculations of heat transfer coefficient of external and internal walls were made. Due to the fact that thermal resistivity calculated as per the formula (4) is known and equal to $R = \delta/\lambda$ [m^{2}K/W], the heat transfer coefficients were determined as per the formulas

$$\propto_{\text{в}} = \frac{\left(\frac{t_{\text{в}} - \tau_{\text{н}}}{t_{\text{в}} - \tau_{\text{в}}} - 1\right)}{R} = \frac{\left(\frac{t_7 - t_2}{t_7 - t_6} - 1\right)}{R}, \tag{5}$$

$$\propto_{н} = \frac{\left(\frac{\tau_{в} - t_{н}}{\tau_{н} - t_{н}} - 1\right)}{R} = \frac{\left(\frac{t_6 - t_1}{t_2 - t_1} - 1\right)}{R} \tag{6}$$

Where $\propto_{в}$, $\propto_{н}$ - heat transfer coefficients of internal and external surfaces respectively, W/(m^2 K); $\tau_{в}$, $\tau_{н}$ – temperatures of enclosing structure internal and external surfaces respectively, ^{o}C; $t_{в}$, $t_{н}$ – temperatures of indoor and outdoor air respectively, ^{o}C; *R* - thermal resistivity , m^2 K/W.

It should be noted that when calculating the heat transfer coefficient, not the average *R* values were used in the formulas (5) and (6) but the current values estimated directly on the basis of temperatures values.

It should be noted that temperature wave passing the wall has the phase of temperature and heat flow oscillations damping, and the experiment data should be taken for calculations considering the phase of temperature wave lagging when passing the enclosing structure mass.

A.M. Shklover presented the damping of temperature and heat flow oscillations as the decrease of harmonic oscillations of temperature and heat flow in the course of wave passing the wall [19]. He also noted zero phase offset between oscillations of temperature and heat flow in the course of wave passing the wall. Temperature oscillations damping from the plane with *x* coordinate till the wall border β for the particular case, when both planes (starting and finishing along the wave movement) are located at the section of regular oscillations, with $Rs \geq 1$, shall be written as follows:

$$\beta = e^{Rs\sqrt{i}} \tag{7}$$

where *s* - periodic penetration depth of the material introduced by O.E. Vlasov, calculated as per the formula

$$s = \sqrt{\frac{2\pi\lambda c\gamma}{z}} \tag{8}$$

where λ - thermal conductivity of material, W/(m^2 K); *c* - specific thermal capacity of material, kJ/(kg K); γ - material density, kg/m^3; z - oscillation period, s;

It should be noted that temperature dumping presented as complex number is very convenient as the number module shows how many times the oscillations amplitude has decreased on the distance under consideration, and the argument shows how much initial phase angles have reduced. Then, the value of temperature oscillations decrease at the regular oscillations section shall be calculated as per the following formula

$$\beta_t = e^{Rs/\sqrt{2}} , \qquad \text{[times]} \tag{9}$$

and the lagging phase shall be calculated as per the following formula

$$\beta_{\varphi} = \frac{Rs}{\sqrt{2}} \quad , \qquad [\text{rad}] \qquad (10)$$

To deduce the above mentioned lagging in hours, it is necessary to use the formula

$$\beta'_{\varphi} = \frac{\beta_{\varphi} Z}{2\pi} \qquad [\text{hour}] \qquad (11)$$

Calculations as per the formulas (10) and (11) allowed to determine the temperature wave and heat flow lagging time: lagging time when passing throughout the wall was equal to 25.4 hours, from t_3 temperature measurement point to the internal wall surface - to 22.6 hours, between t_3 и t_5 temperature measurement points - to 5.1 hours, q value was determined with the offset of 22.6 hours at that.

The calculated values of heat transfer coefficients of external and internal surface are given in the form of graphs shown at the Figure 5. The average coefficient values as per 1000 reference points were assumed: for internal surface 9.1 W/(m^2 K), for external surface 5.1 W/(m^2 K). It is possible that the surface heat transfer coefficient on inside of the wall is larger than on the outside as the studied wall was in terminal, air flow was absent.

Considering the interim calculations shown above, the values of temperature in cross sections of the external building wall at the depth of 85, 185 and 280 mm from external surface were calculated with the use of the developed method based on finite differences and compared with actual temperatures in these cross sections measured during the experiment. Figure 6 shows calculated and experimental graphs at the minor time interval of 12 days. During this interval the external temperature grew abruptly after reaching the minimum, after which it was changing more smoothly. The calculated values with the good convergence repeated the experimental curves in all sections at that.

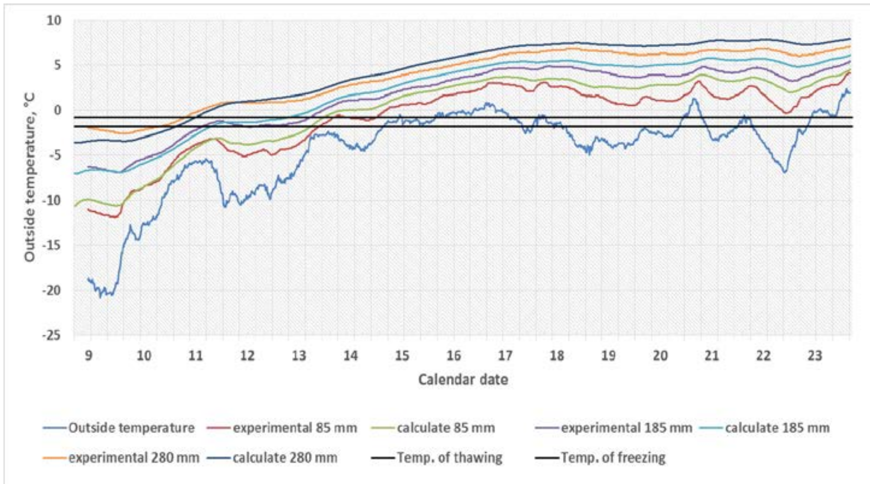

Fig. 6. Comparison of the calculated and experimental values of temperature distribution in various sections of the exterior walls of the building.

3 Method for Calculating Year Temperature Intensity Parameter for Walls with Various Structures and Results Analysis

Analysis of results on the number of freezing and thawing cycles in various external wall cross-sections in nonsteady process given in the Table 1 allows to proceed to thermal forces analysis on the studied structure.

Important parameter N_i, which characterizes the thermal impact on enclosing structure of the building taking into account global temperature changes, defines number of freezing and thawing cycles in all external wall sections during *i*-th year. This parameter is called "year temperature intensity" for external wall structure and it characterizes the impact on this structure caused by outdoor temperature changes. "Year temperature intensity" parameter links outdoor air characteristics: temperature changes caused by climate changes, and changes in the number of cycles of temperature transition through with technical specifications of the enclosing structure: thickness and thermophysical properties of the structure material.

Year temperature intensity graph for external walls of solid common bricks with thickness 510 mm N_i, was constructed based on the analysis of temperature distribution graphs similar to the one in Figure 3, and it is shown in the Figure 7. For further calculations convenience, the year 1900 was taken as the zero point on X-axis.

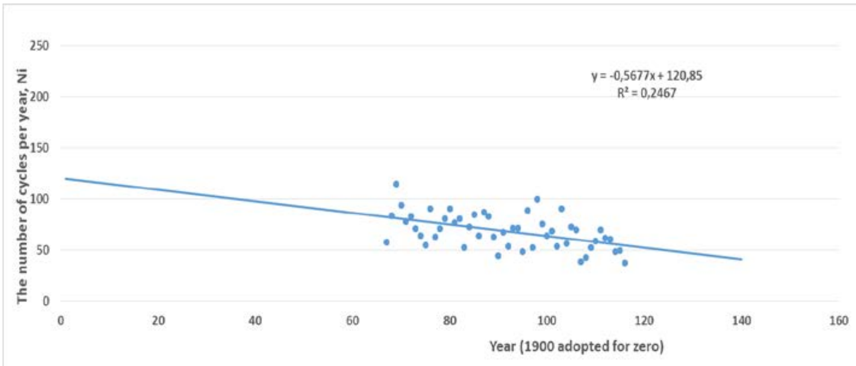

Fig. 7. The number of cycles of the transition temperature of zero in all the estimated cross sections of the outer walls of solid red brick with a thickness of 510 mm *Ni* (temperature the intensity of years for this material).

The graph in Figure 7 demonstrates that distribution of value N_i – year temperature intensity – follows simple negative linear regression.

The correctness of our applying the linear regression for describing the year temperature intensity can be analyzed with the help of residual analysis statistical method - the graphic method allowing to evaluate the accuracy of the regression model. It is possible to reveal the potential noncompliances with the regression analysis conditions. Residue, or error of estimate, is the difference between the observed and forecasted values of dependent variable under the given value of variable x.

To evaluate the applicability of regression empirical model, the residues shall be singled out in the vertical axis and x values — on the horizontal axis. In case the empirical model is applicable, the graph should not display the explicit regular pattern. But in case the empirical model is not applicable, the figure will show the dependence between x values and residues. It is evident from the graphic residual analysis made by us that the distribution of residuals is chaotic and does not display the regular pattern (Figure 7a). Residuals often have both positive and negative values. This allows to conclude that the linear regression model is applicable for solving the problem.

Graphs on the figures result from the calculation of the number of cycles of freezing and thawing, and the number of cycles of freezing and thawing in per cent of the total number of cycles per year in the cross section at 25 mm from the external wall surface. The same graphs were constructed for the calculated cross sections of the external building wall structure.

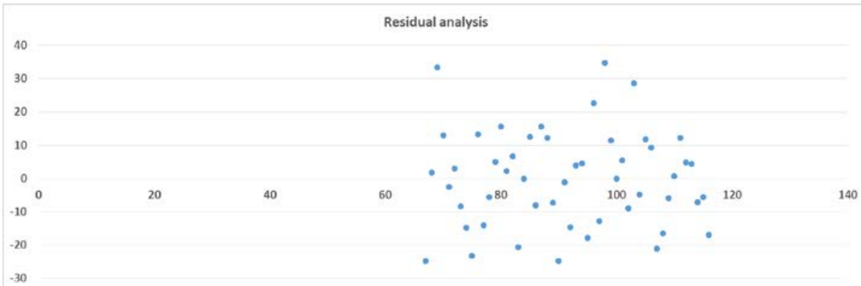

Fig. 7a. The residual analysis of the graphic in Figure 7.

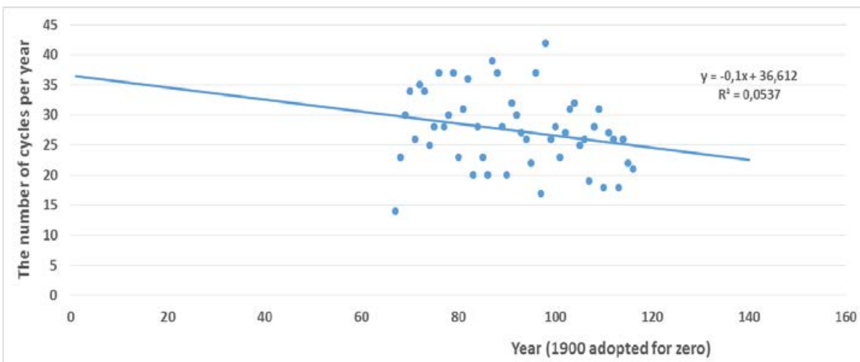

Fig. 8. Changing the number of cycles of freezing and thawing per year in the cross-section 25 mm from the outer surface of the wall.

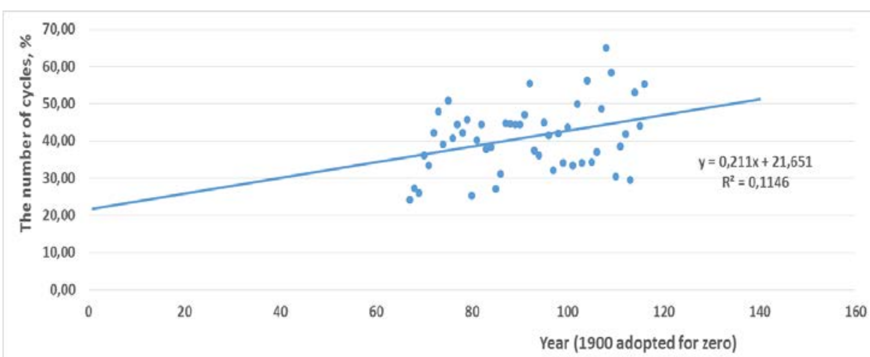

Fig. 9. Changing the number of cycles of freezing and thawing, in percent of the total number of cycles per year, in the cross-section 25 mm from the outer surface of the wall.

4 Analysis of Temperature Impact on Enclosing Structures

At the moment, the evaluation of possibility to use a particular design of external building wall from the viewpoint of its durability is made on the basis of various parameters, such as thermal conductivity, structure humidifying, freeze-thaw resistance. The conclusion on the structure suitability is made on the basis of these parameters in their totality. However until now there was no numeric parameter used to provide the integral evaluation of the temperature impact on enclosing structure.

Let us consider the efficiency of the developed method for evaluation of temperature impact on external walls of the following structure: bearing external wall of the building is made of red loan brick and has the thickness of 510 mm and 700 mm. External wall is reinforced with mineral isolation plates with thickness of 100 mm and thermal conductivity of 0.05 W/(m K) on the internal side. This structure is applicable, for example, for reconstruction of old buildings with lofts arrangement.

For each structure, the graphs similar to that on Figure 3 are plotted, analysis results are summarized in tables similar to Table 1, based on which graphs for each combination are plotted similarly to those shown on Figures 8 and 9.

As it was mentioned before, to analyze the temperature impact on the enclosing structure considering the global climate change, we have introduced the year temperature intensity parameter. On Figure 10 the year temperature intensity graphs are shown for the 510 mm external wall structure with thermal insulation on the internal side and without it. It is evident than in case of the wall with no thermal insulation the polythermal load on the wall will reduce in time, and for the structure with inner thermal insulation it will grow. In case of the external wall structure with no thermal insulation the reduction of freezing and thawing cycles is explained with the fact that the global warming influence (Figure 1) impacts the external wall more than the certain increase of cycles of outdoor temperature transitions through zero shown on Figure 2.

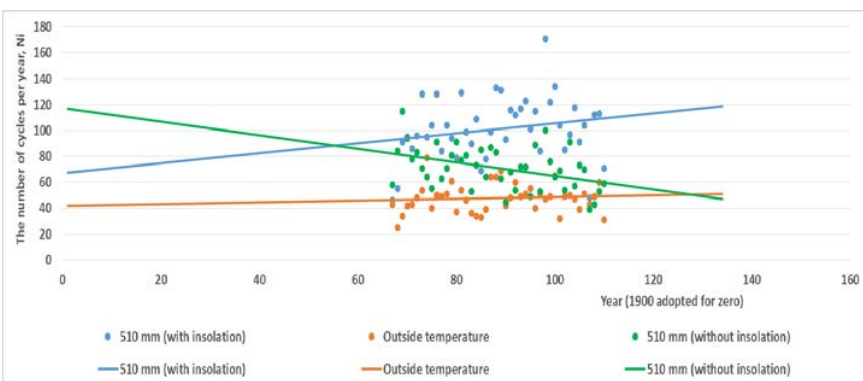

Fig. 10. Graphs of intensity of temperature of the year (*Ni*) for exterior brick walls 510 mm with and without insulation.

This conclusion is confirmed by freezing and thawing graphs as per the structure cross sections plotted similarly to those shown on Figures 8 and 9. For convenience of analyzing, the characteristics of the linear regression graphs are shown in the Table 2.

Table 2. Characteristics of Linear Regression Graphs for Wall with Brickwork Thickness of 510 mm.

Coordinate of external wall cross-section	Graph type	Coefficients of linear regression graphs *y = ax + b (with insulation)*		Coefficients of linear regression graphs *y = ax + b (without insulation)*	
		a	*b*	*a*	*b*
25	Number of cycles	0,10	13,17	- 0,10	36,61
	% of the total number of cycles	0,21	21,65	0,21	21,65
75	Number of cycles	0,12	4,84	- 0,19	36,13
	% of the total number of cycles	0,21	21,65	-0,08	34,47
125	Number of cycles	0,12	1,98	- 0,19	32,02
	% of the total number of cycles	0,08	4,67	- 0,12	30,86
175	Number of cycles	0,06	4,69	- 0,05	11,58
	% of the total number of cycles	0,03	6,99	0,01	8,98
225	Number of cycles	0,02	5,86		
	% of the total number of cycles	-0,0005	7,85	- 0,02	3,88
275	Number of cycles	0,007	6,16		
	% of the total number of cycles	-0,02	8,56		
325	Number of cycles	0,005	5,30		
	% of the total number of cycles	-0,02	7,64		
375	Number of cycles	-0,003	5,48		
	% of the total number of cycles	-0,03	8,27		
425	Number of cycles	-0,004	5,47		
	% of the total number of cycles	-0,04	8,42		
	Number of cycles	-0,01	6,58		

475	% of the total number of cycles	-0,05	9,58		
	Number of cycles	-0,03	7,80		
510	% of the total number of cycles	-0,06	10,08		

It is evident that in the structure with internal thermal insulation the coefficient *a* is much more than zero for sections up to 175 mm from the external wall surface, which indicates the increase of the number of freezing and thawing cycles in these sections as time passes. For sections of 225 mm to 425 mm the coefficient *a* is close to zero, i.e. the number of cycles in these sections is almost constant; for sections of 475 mm and 510 mm *a* is less than zero, the number of cycles decreases, which confirms the conclusion on the decrease of brickwork freezing depth due to the global warming.

For the brick wall without thermal insulation, coefficient *a* is negative for all cross sections, which determines the decrease of number of freezing and thawing cycles throughout the external wall.

The bar graph in the Figure 11 makes it possible to compare the distribution of the number of freezing and thawing cycles in various cross sections of the brickwork with the thickness of 510 mm with thermal insulation on the internal side and without it. It is important to note that in the brickwork cross sections located closer to the external surface, the number of freezing and thawing cycles is much lower for the structure with thermal insulation, than for the structure without thermal insulation on the internal side of the wall.

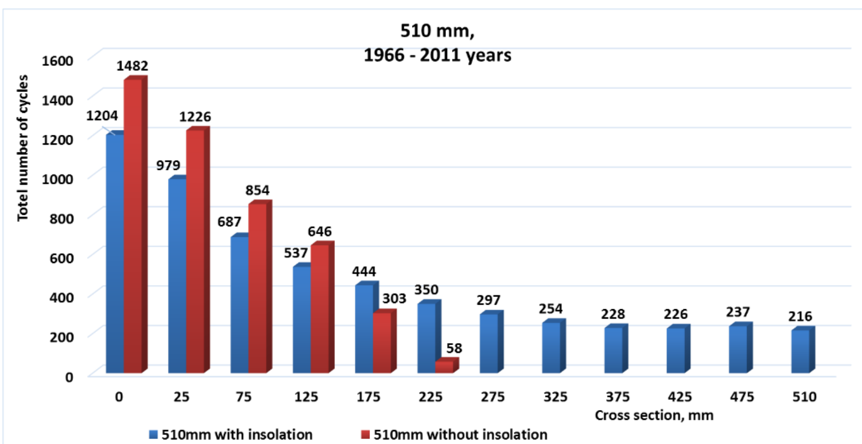

Fig. 11. The number of cycles of freezing and thawing in the cross section of the exterior brick walls with thickness of 510 mm 1966-2011 years.

It is important to note that the zone of the maximum brickwork humidifying is considered to be the zone in the first third from the external surface of the enclosing structure, i.e. for sections up to 125 mm. In these sections, for the structure with thermal insulation 3407 freezing and thawing cycles will take place in the reference period, and for the structure with no thermal insulation - 4208 cycles, i.e. 23.5% more. In the brickwork sections located deeper in the structure with thermal insulation, the number of freezing and thawing cycles will be minor and rather constant, i.e. the certain redistribution of the cycles number throughout the brickwork cross-section will take place with the decrease of the load in external sections to internal ones. It can be defined that 61% of all brickwork freezing and thawing cycles in the reference period will take place in the sections located in the first third of the enclosing structure section in case the internal surface is insulated. For the structure with no thermal insulation this parameter will be equal to 92%.

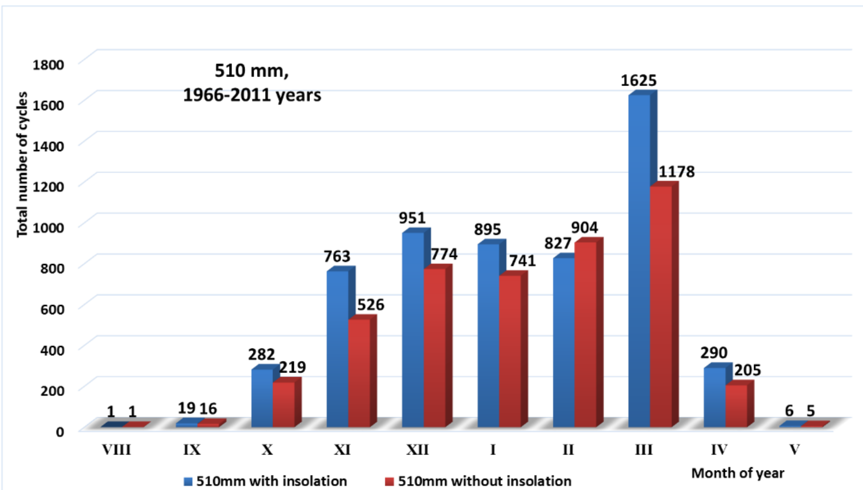

Fig. 12. The number of cycles of freezing and thawing of the exterior brick walls with thickness of 510 mm in 1966-2011 years by month.

Figure 12 shows the bar graph for comparing the number of brickwork freezing and thawing cycles for the structure with thermal insulation and without it with breakdown per months. In general, this bar graph confirms the conclusions made earlier, however it gives the data on temperature impact in various months of the year. This is important to know, because the maximum structure humidifying due to the diffusive moisture accumulation occurs in March – April [20-26]. It is evident that in March the number of freezing and thawing cycles for the structure with thermal insulation is 1625 instead of 1178 cycles for the structure without thermal insulation, which is 38% more.
The graphs of the year temperature intensity parameter change for the structure of external wall with 700 mm thick brickwork and without thermal insulation are shown in Figure 13. In terms of pattern, these graphs repeat the graphs for 510 mm brick wall

structure, which confirms the correctness of conclusions made concerning the previous structure.

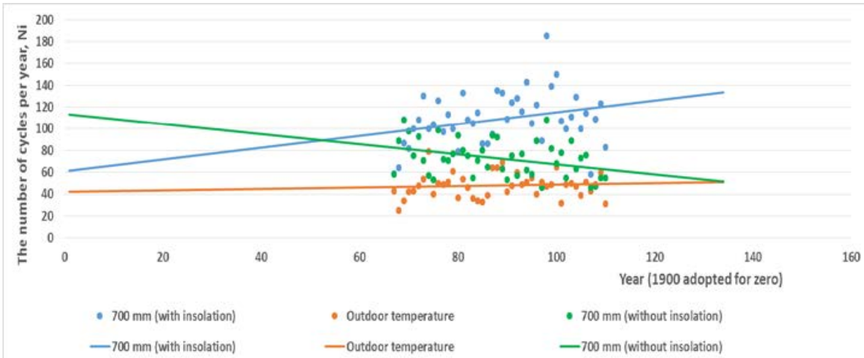

Fig. 13. Graphs of intensity of temperature of the year (Ni) for exterior brick walls 700 mm with and without insulation.

Characteristics of linear regression graphs are shown in the Table 3.

Table 3. Characteristics of Linear Regression Graphs for Structure with Brick Wall Thickness of 700 mm.

Coordinate of external wall cross-section	Graph type	Coefficients of linear regression graphs *y = ax + b (with insulation)*		Coefficients of linear regression graphs *y = ax + b (without insulation)*	
		a	*b*	*a*	*b*
25	Number of cycles	0,13	10,91	0,02	20,65
	% of the total number of cycles	0,21	21,65	0,21	21,65
75	Number of cycles	0,13	3,66	-0,07	21,58
	% of the total number of cycles	0,21	21,65	0,21	21,65
125	Number of cycles	0,14	-0,16	-0,14	25,36
	% of the total number of cycles	0,08	4,01	-0,08	25,05
175	Number of cycles	0,08	2,45	-0,12	20,35
	% of the total number of cycles	0,04	4,98	-0,09	20,79
	Number of cycles	0,06	3,20	-0,03	9,37

225	% of the total number of cycles	0,02	5,57	0,01	7,87
275	Number of cycles	0,008	5,92	-0,04	7,02
	% of the total number of cycles	-0,02	7,71	-0,01	6,23
325	Number of cycles	0,03	2,57	-0,06	7,00
	% of the total number of cycles	0,005	4,14	-0,07	7,97
375	Number of cycles	0,04	1,04	-0,02	2,10
	% of the total number of cycles	0,02	2,61	-0,02	2,43
425	Number of cycles	0,02	2,31		
	% of the total number of cycles	-0,004	4,01		
475	Number of cycles	0,005	3,47		
	% of the total number of cycles	-0,02	5,46		
525	Number of cycles	-0,01	4,70		
	% of the total number of cycles	-0,03	6,54		
575	Number of cycles	-0,01	4,75		
	% of the total number of cycles	-0,04	6,59		
625	Number of cycles	-0,02	5,37		
	% of the total number of cycles	-0,05	7,25		
675	Number of cycles	-0,03	5,94		
	% of the total number of cycles	-0,05	7,38		
700	Number of cycles	-0,02	5,00		
	% of the total number of cycles	-0,04	6,28		

It should be noted that the number of cycles of freezing and thawing for structure with thermal insulation increases up to 425 mm cross section as time passes, coefficient *a* is almost equal to zero in the cross section 475, i.e. the number of cycles in this section is constant during a year, and starting from the cross section at 525 mm the number of cycles of freezing and thawing decreases. For the structure with 700 mm brick wall without thermal insulation, the number of cycles of freezing and thawing for the cross section at 25 mm will increase as well; starting from the section at 75 mm from the external wall surface the number of cycles will decrease as time passes.

When considering the bar graph showing the number of cycles of freezing and thawing in various sections of 700 mm thick brickwork with thermal insulation and without it (Figure 14), it is necessary to note a certain difference for structures with brick wall thickness of 510 mm and 700 mm. If the number of cycles of freezing and thawing for the structure with 510 mm brick wall was 23.5% less for the structure with thermal insulation, for the structure with 700 mm brick wall the number of cycles in the first triens is almost the same for the structure with thermal insulation and without it. In the deeper layers of the structure, the number of freezing and thawing cycles is also constant and minor, same as for the structure with 510 mm brickwork.

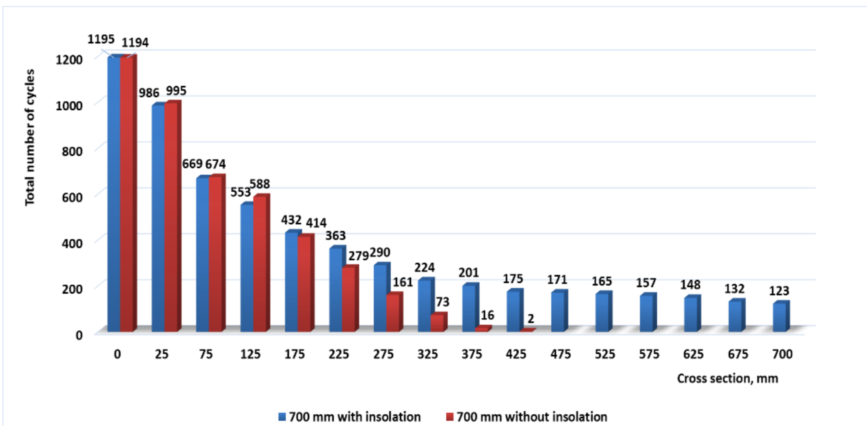

Fig. 14. Distribution of the number of cycles of freezing and thawing on the cross section of the exterior brick walls 700 mm with and without insulation in 1966 – 2011.

The developed method allows to analyze the dynamics of temperature impact on enclosing structure in the course of time. Figure 15 shows the calculated data on the number of freezing and thawing cycles as per brickwork cross sections for the enclosing structure with 510 mm brickwork with thermal insulation on the internal side and without it, in the period since 2011 till 2055. It is evident that the impact on enclosing structure, especially in the first triens as per the brickwork cross section, changes abruptly versus the basic reference period of temperature impact calculation since 1966 till 2011 (Figure 11). During the basic reference period the number of freezing and thawing cycles for the structure with thermal insulation in sections within the first triens of the enclosing structure cross section was lower than that for the structure without thermal insulation, however in the period since 2011 till 2055 the number of freezing and thawing cycles in the first triens of cross section of the enclosing structure with thermal insulation is 2853 freezing and thawing cycles, and for the structure without thermal insulation - 1787, i.e. 59.7% less. In 2011 - 2055, 55.0% of all brickwork freezing and thawing cycles in the reference period will take place in the sections located in the first third of the enclosing structure section in case the internal surface is insulated. For the structure with no thermal insulation this parameter will be equal to 89,8%.

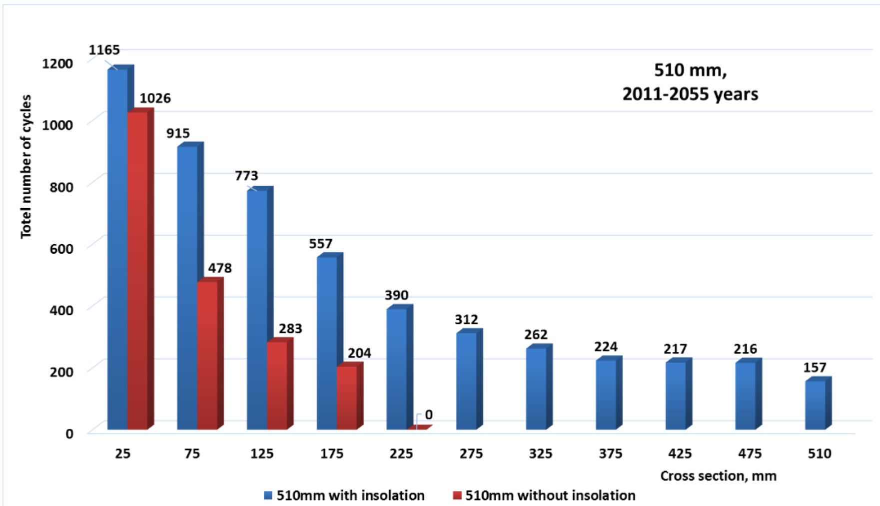

Fig. 15. Distribution of the number of cycles of freezing and thawing on the cross section of the exterior brick walls 700 mm with and without insulation in 2011 – 2055.

Conclusions

The method has been developed for calculating the temperature distribution over the cross section of enclosing structure under nonsteady heat transfer conditions. The method allows determining the number of cycles of freezing and thawing in each cross section of the external building wall with a high degree of confidence.

Field study on the method in combination with developed technique for processing results obtained in the field conditions have demonstrated good convergence of calculated temperature with actual temperature measured in various sections of the external building wall.

The developed method for analyzing the results of heat distribution calculation at a cross-section of the external building wall allowed to get the numerical characteristics of the change in temperature impact on various enclosing structures and to define he dynamics in the change of temperature impact per the structure cross section in the next 50 – 100 years interval. The authors' introducing the "Year Temperature Intensity" parameter allowed to link the outdoor air characteristics: temperature changes caused by climate changes, and changes in the number of cycles of outdoor temperature transition through with technical specifications of the enclosing structure: thickness and thermophysical properties of the structure material.

The method ensures the ample opportunities for analyzing the durability of various enclosing structures, for example concrete walls, taking into account the adaptation to the global climate change.

Yes, the study can be use for any types of envelopes and now we use it for concrete walls, for example.

References

1. The second assessment report on climate change and their consequences on the territory of the Russian Federation / VM Katsov, SM Semenov. - Moscow: Roshydromet, 2014. - 58 p.
2. IPCC Fifth Assessment Report. WG II Report “Climate Change 2014: Impacts, Adaptation and Vulnerability”. IPCC, 2014.
3. LEG. 2012. National Adaptation Plans. Technical Guidelines for the National Adaptation Plan Process.
4. An array of average monthly air temperature data at Russian stations / Bulygina, ON, Razuvaev VN, Trofimenko LT, et al Obninsk: VNIIGMI-WDC, 2016. / [Electronic resource] Access mode: http: //www.meteo.ru/climate/sp_clim.php.
5. Russian hydrometeorological portal. Hydrometeorological data of the Russian State Data Foundation on the state of the natural environment. http://meteo.ru/.
6. SP 20.13330.2011 "Loads and effects (updated version of SNiP 2.01.07-85 *)."
7. SP 131.13330.2012. "Set of rules. Building climatology. (Updated version of SNiP 23-01-99 *) "
8. Vlasov O.E. Flat heat waves. - Izvestiya teplotehnicheskogo institut. 1927, vol. 3 (26).
9. Fokin K.F. Building thermophysics of enclosing parts of buildings. - M .: ABOK-press. 2006. - 256 pages.
10. Miller L.G. Calculating Vapor and Heat Transfer Through Walls. // Heat. Ventil. - 1938. - Vol. 35. - No. 11. - P. 56-58.
11. Carslow H.S., Jaeger J.C. Conduction of Heat in Solids. - Oxford, 1959.
12. Crank J. The Mathematics of Diffusion. - Oxford, 1975. - 414p.
13. Buxuan W., Zhaohong F. A theoretical study on the heat and mass transfer in wet porous building materials. // J. Eng. Thermophys. - 1985. - Vol. 6. - No. 1. - P. 60-62.
14. De Vries Daniel A. The theory of heat and moisture transfer in porous media revisited. // Int. J. Heat Mass Transfer. - 1987. - Vol. 30. - No. 7. - P. 1343-1350.
15. Kerestecioglu A. et al. Theoretical and Computational Investigation of Algorithms for simultaneous Heat and Moisture Transport in Buildings. - Florida, 1989.
16. Hu J.-T., Ren X.-H., Zhao F.-Y., Liu D., Wang H.-Q. Natural convective heat and moisture transfer in an inclined building enclosure with one slender wall of finite thickness: analytical investigation and non-unique steady flow solutions // International Journal of Heat and Mass Transfer. 2017. T. 104. C. 1160-1176.
17. Zheldakov, D. Y., Frolov A. A., Ivanov S. Y. Investigation of strength of masonry walls in the building Kadashevsky baths // Building materials. 2016. No. 6. P. 55-57.
18. Zheldakov D.Y., Frolov A.A. Segment method for calculating the temperature distribution along the section of the enclosing building structure // Housing construction. 2017. № 6. P. 36-39.
19. Shklover A.M. Heat transfer with periodic thermal effects. - M .: Gosenergoizdat.1952. 98 pages.
20. Gagarin VG, Pastushkov P.P. Determination of the calculated humidity of building materials / / Industrial and civil construction. 2015. № 8. P. 28-33.

21. Gagarin V. G., Kozlov V. V., Zubarev K. P. Analysis of the location of maximum moisture in building envelopes with different thickness of the insulating layer // Housing construction. 2016. No. 6. P. 8-12.
22. Bomberg M. Moisture flow through porous building materials. Lund Institute of Technology. - 1974. - Report No. 52. - 188p.
23. Andersson A.C. Verification of Calculation Methods for Moisture Transport in Porous Building Materials. - Lund, 1985.
24. Everett D.H. The thermodynamics of frost damage to porous solids. // Trans. Faraday Soc. - 1961. - Vol. 57. - Pt. 9. - P. 1541-1551.
25. Gray W.G. A derivation of the equations for multi-phase transport. // Chem. Eng. Sci. - 1975. - Vol. 30. - P. 229-233.
26. Berger J., Mendes N., Dutykh D. On the optimal experiment design for heat and moisture parameter estimation // Experimental Thermal and Fluid Science. 2017. T. 81. C. 109-122.